DISCLAIMER

This report was prepared as an account of work sponsored by an agency of the United States Government. Neither the United States Government nor any agency thereof, nor any of their employees, makes any warranty, express or implied, or assumes any legal liability or responsibility for the accuracy, completeness, or usefulness of any information, apparatus, product, or process disclosed, or represents that its use would not infringe privately owned rights. Reference herein to any specific commercial product, process, or service by trade name, trademark, manufacturer, or otherwise does not necessarily constitute or imply its endorsement, recommendation, or favoring by the United States Government or any agency thereof. The views and opinions of authors expressed herein do not necessarily state or reflect those of the United States Government or any agency thereof. Reference herein to any social initiative (including but not limited to Diversity, Equity, and Inclusion (DEI); Community Benefits Plans (CBP); Justice 40; etc.) is made by the Author independent of any current requirement by the United States Government and does not constitute or imply endorsement, recommendation, or support by the United States Government or any agency thereof.

Project Report ORNL/SPR-2025/3685

Oak Ridge National Laboratory

The Maintainable Fusion Pilot Plant

Venugopal K Varma
Andrzej Nycz
William Carter
Michael Kirka
Christopher Masuo
Dustin Ottinger
Juergen Rapp
Brad Sampson
Michael Sebok
Jeremy Slade

December 2024

OAK RIDGE National Laboratory

U.S. Department of ENERGY

ORNL IS MANAGED BY UT-BATTELLE LLC FOR THE US DEPARTMENT OF ENERGY

ORNL/SPR-2025/3685

Fusion Energy Division

The Maintainable Fusion Pilot Plant

Venugopal K Varma
Andrzej Nycz
William Carter
Michael Kirka
Christopher Masuo
Dustin Ottinger
Juergen Rapp
Brad Sampson
Michael Sebok
Jeremy Slade

December 2024

Prepared by
OAK RIDGE NATIONAL LABORATORY
Oak Ridge, TN 37831
managed by
UT-BATTELLE LLC
for the
US DEPARTMENT OF ENERGY
under contract DE-AC05-00OR22725

Table of Contents

List of Figures

List of Tables

ABBREVIATIONS AND ACRONYMS

AM	Additive Manufacturing
CX	Charge Exchange
cRIO	Compact Remote Input Output
FNSF	Fusion Nuclear Science Facility
FPP	Fusion Pilot Plant
GMAW	Gas Metal Arc Welding
ITER	The Way (previously International Thermonuclear Experimental Reactor)
MDF	Manufacturing Demonstration Facility
MEMS	Micro Electromechanical Systems
NASEM	National Academies of Science, Engineering, and Medicine
NI	National Instruments
ORNL	Oak Ridge National Laboratory
PAW	Plasma Arc Welding
PFC	Plasma Facing Components
RAMI	Reliability, Availability, Maintainability and Inspectability
WAAM	Wire Arc Additive Manufacturing

ABSTRACT

1. BACKGROUND

The US fusion community has coalesced around the goal of building an FPP as described by the National Academies of Science, Engineering, and Medicine (NASEM) [1]. In addition to demonstrating the viability of the technologies necessary to operate such a plant, including demonstration of net energy and electricity production, NASEM found that a "fusion pilot plant will need to demonstrate the ability to efficiently perform remote maintenance and replacement in support of the design of a power plant, taking into account details of the consequences of the fusion environment, such as material activation and tritium retention in components." Current designs of fusion demonstration reactors do usually foresee a regular exchange of their first wall modules, including the tritium breeding blankets. In the European Power Plant Conceptual Studies [2], it is assumed that a fusion reactor will need to change its divertor every 2 years and its first wall blanket module every 5 to 6 years to reach acceptable availability. Underlying this capability are remote-handling technologies to keep the outage for the exchange of these components short. There are many uncertainties in the remote-handling schemes, and most schemes are at a preconceptual level at best. In addition, the exchange of these components would either produce an enormous rad-waste stream or would require an enormous refurbishment activity with huge cost-prohibitive hot-cells. Past Fusion Nuclear Science Facility (FNSF) preconceptual studies [3] have led to hot cell dimensions of an unbelievable size, likely costing tens of billions of dollars. Already at The Way (previously International Thermonuclear Experimental Reactor, ITER), hot-cells have become cost-prohibitive, demanding redesigns of the ITER first wall to reduce the toxic rad-waste/inventory [4].

In this in-situ PFC repair project, a concept for a long-life, maintainable first wall module concept is developed and tested. This first wall concept relies on innovative remote handling to repair the first wall modules in-situ, avoiding costly refurbishments outside of the tokamak vessel. This approach was highlighted in the Fusion Energy Sciences Advisory Committee (FESAC) report on *Transformative Enabling Capabilities for Efficient Advance Toward Fusion Energy* [5]. In general, the damage of the first wall armor is due to particle and radiation exposures. Load conditions vary from one fusion reactor design to another. In tokamaks, first wall Plasma Facing Components (PFCs) are exposed to far-Scrape-Off-Layer plasma fluxes, electromagnetic radiation, energetic CX neutrals, and potentially runaway electron beams. Protecting the first wall to the worst-case load conditions would require the design of a very thick first wall armor. Transient heat and particle fluxes due to disruptions or edge localized modes can lead to excessive heat loads resulting potentially in melting PFCs down to the cooling channel. Catastrophic events like these need to be avoided by appropriate disruption mitigation systems [6]. However, failure of these systems will still put a first wall at an unacceptable risk. Hence, a first wall design needs to accommodate the occasional transient heat loads by introducing sacrificial limiters, which will absorb these transients.

The blanket module will be radially recessed from these limiters. The armor of the blanket module needs to be thin to allow neutrons to transmit most of their power to the breeding blanket and to allow an efficient heat transfer from the amor to the first wall coolant. Effective limiters will thus eliminate the plasma fluxes altogether to the blanket armor, and only high energetic CX neutral fluxes, electromagnetic radiation and neutron fluxes will impinge on the blanket armor. While such a design will be resilient to most loads, localized electromagnetic radiation during a thermal quench of a disruption might still lead to thermal loads unmanageable for the blanket armor. Thus, some damage of the blanket armor cannot be excluded. In-situ repair of the thin first wall armor is an attractive option to avoid costly and lengthy replacements of the blanket modules. In this project, an in-situ repair technique is being developed based on an AM module deployed on a remote-handling arm. In addition, radiation-hardened in-situ diagnostics is being developed to inform on the status of the first wall. MEMS-based diagnostics will be embedded in the PFC to deliver

the incident CX-neutral flux and armor-thickness measurements. Again, this is in response to the FESAC report on *Transformative Enabling Capabilities for Efficient Advance Toward Fusion Energy* [5].

This report summarized the progress made during the first year of research. The initial quarter was used in selecting components and obtaining quotes, while in the 2nd quarter many of the purchases were made. In the third quarter, most of the items were assembled, the fourth quester, testing started. A test stand was also fabricated to prove the deposition of tungsten in any orientation. During the 4th quarter testing of deposition with 410 Stainless Steel (SS) was completed using both TIG and Plasma torches.

2. METAL ADDITIVE REPAIR OF PLASMA FACING COMPONENTS

2.1 INTRODUCTION

An energy generating fusion reactor will need efficient methods for periodic maintenance and inspection of neutron irradiated components. The importance of Reliability, Availability, Maintainability and Inspectability (RAMI) was recognized in the CPP/FESAC [6,7] reports in order to be able to construct and operate a fusion nuclear facility like the Fusion Pilot Plant. The fusion environment is very harsh, involving severe plasma, neutron and gamma ray loading all components in the fusion core during operation. When the plasma is off, the only remaining load is gamma radiation, which can be quite high in the first wall at ~ 5 x 10^5 Sv/hr (compared to allowed exposures of 20 mSv/yr for workers and 1 mSv/yr for the public) and will decrease to ~ 8 x 10^4 Sv/hr after 1 day to 1 week [8]. The corresponding first wall decay heat begins at 4 x 10^5 W/m^3 which drops to ~ 10^4 W/m^3 after a similar amount of time. Energetic particles cause damage to the surfaces of the tokamak plasma facing components.

So, maintenance and repair have to be performed under the radiation and heat load mentioned above. Any method to perform these tasks fast will increase the reliability of the fusion device. The plasma facing surfaces will undergo erosion due to the energetic particles that it will be exposed to. Removing damaged components and replacing them will be both time consuming and costly. Instead, if an in-situ repair can be envisioned for these components, the maintenance time cane be considerably reduced. Metal Additive Manufacturing (AM) is one way to in-situ repair the PFCs.

2.2 METAL ADDITIVE MANUFACTURING OPTIONS

There are many methods for metal AM, but not all are feasible for in-situ metal deposition. Table 1. Describes the methods currently in use for metal AM and their characteristics.

Table 1. Metal additive Manufacturing Methods

Method	Requirements	In-Situ Compatible	Selected
Printing & Sintering	This is a multi-step process where the material once printed has to undergo a sintering process	No	No
E-Beam	The feed can be either powder or wire, but requires a vacuum	No (difficult to make vacuum in-situ)	No
Laser	Feed can be either wire or powder.	Yes (the laser head failure rate is high with high replacement cost)	No
Wire Arc	MIG, TIG, or Plasma. MIG creates impurities and cannot support the surface finish requirements	Yes	Yes (TIG and Plasma being pursued)

So, although there are multiple metal deposition methods, only wire arc and laser could potentially be used as method for in-situ repair. Due to potential problems with laser, wire arc was chosen for the in-situ repair of Plasma Facing Components.

2.3 METAL ARC DEPOSITION

To quickly start the research and obtain some preliminary results, the project got started at the Manufacturing Demonstration Facility (MDF) which has several metal AM systems in operation. MDF's MedUSA facility uses a common rotating platform where three independent cooperative robots can AM print a single part while coordinating their motions and the amount of metal to deposit. The MIG welder that was attached to the robot was changed to a TIG welder for precision and more controlled deposition rate.

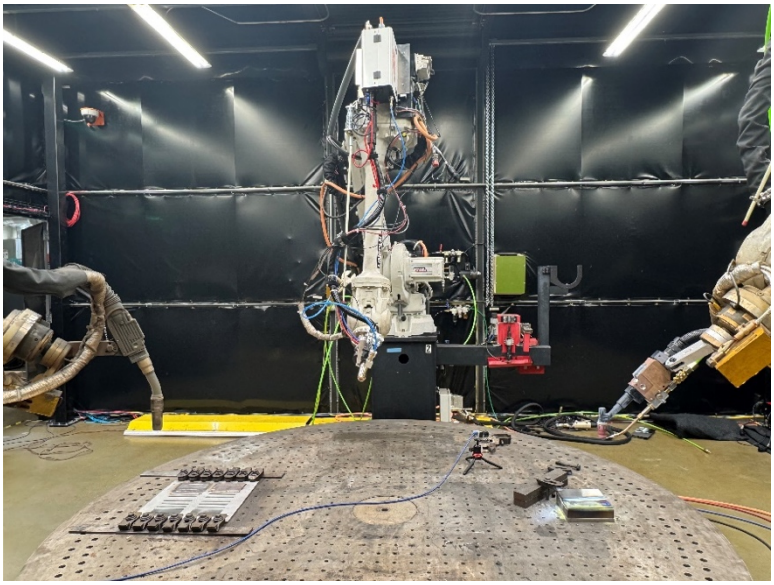

Figure 1. The MedUSA System equipped with a plasma torch for the robot in the middle and a TIG torch for the robot on the right, and MIG on left

2.3.1 Preliminary Testing

One of the first tasks performed was to ascertain whether the existing set-up at MDF could be used for metal arc deposition of tungsten. So, without any additions to the existing MedUSA wire arc additive manufacturing (WAAM) cell, the existing gas metal arc welding (GMAW) torches were evaluated on their ability to deposit tungsten wire onto steel and tungsten substrates. Beads were deposited using a Abicor-Binzel Robo WH W 600 GMAW torch powered by a Lincoln R450 power supply. A short tungsten bead was deposited using 0.035" pure tungsten wire from Midwest Tungsten onto a mild steel substrate using the settings shown in Table 2. Initial results demonstrated that, while tungsten could be deposited using the existing GMAW torches, it was highly difficult to maintain a stable bead. There was a large volume of spherical tungsten spatter generated, and the surface of the bead was inconsistent compared to a nominal deposition. Additionally, the extreme heat required to melt tungsten also tended to melt the copper contact tips used in GMAW deposition. This limited the deposition of tungsten to relatively short beads before the contact tip would melt.

Table 2: Welding Parameters for GMAW Tungsten Deposition

Weld Mode	Current	Voltage	Travel Speed	Wire Feed	Gas Mixture
296	100 A	30 V	2 mm/s	42 mm/s	100% He

Figure 2: Initial testing of tungsten wire deposited on a mild steel substrate

In addition to the testing of tungsten deposited on a steel substrate, testing was also performed using tungsten wire deposited onto a pure tungsten substrate. However, in this case, there was no successful adhesion of tungsten onto the tungsten substrate. Welding power was increased until the contact tips melted within the first few seconds of welding without any melting of the tungsten substrate. The tungsten wire formed an unstable bead on top of the substrate, but there was almost no adhesion between this bead and the plate below. With these results in mind, it was clear that alternative welding methods should be explored to enable stable tungsten deposition.

2.3.2 System Selection

In order to successfully deposit tungsten wire onto a tungsten substrate, it was necessary to select appropriate welding equipment that could maintain the temperatures required to melt tungsten without damage to the welding equipment. It was determined that both gas tungsten arc welding (GTAW) and Plasma Arc Welding (PAW) equipment would potentially be suitable for tungsten deposition. Both GTAW and PAW equipment were integrated in order to compare their relative strengths and weaknesses in the repair of plasma facing components. Specifically, GTAW is the more widely researched welding process with a demonstrated ability to deposit tungsten wire [9] while the PAW process generates a highly focused welding arc and reduced thermal shock when compared to GTAW. Initially, these processes would be validated via installation on the existing multi-robot MedUSA additive manufacturing cell with later testing being performed on a custom robotic welding cell used to demonstrate PFC repair.

After reviewing the existing literature and doing preliminary calculations, it was estimated that a suitable arc welding setup should be capable of generating at least 300A of current or more to ensure a consistent tungsten deposition. Other key factors to consider were the price of a complete system, the automation interfaces available for communication, and the expected difficulty of system integration. Welding torches and power supplies were independently analyzed, but priority was given to systems with a combined power supply/torch package to simplify integration. Selection of an appropriate GTAW system was influenced by the nascent support of the preexisting Lincoln Electric R450 robotic welders for high frequency GTAW welding with the appropriate add-on. This allowed GTAW welding to be added to MedUSA through the addition of a Lincoln Electric Advanced Module to generate a high frequency starting current along with the selection of a suitable GTAW torch. The two torches selected were a Lincoln Electric TopTig torch and an Abicor-Binzel Abitig WH 400 W. The Abicor-Binzel torch was selected for its similarity to the existing GMAW torches and its high current limits. Comparatively, the

TopTig torch was selected for its unique, nearly vertical wire feeding angle and the potential for improved additive deposition quality.

For the PAW system, six potential system candidates were identified, and they are summarized in Table 3. After reviewing the systems available, a decision was made to select two systems based on independent considerations. The first system would be a low-cost system with limited automation that could be rapidly integrated and tested. The second system would be a system with full automation and advanced functionality that would offer enhanced control of the deposition process. The low-cost systems from Precision Welding Technologies, Profusion, and Sanrex were considered for the first selection with the Profusion plasma console being the final selection. The Profusion system was unique in that it would act as an add-on module to the existing Lincoln R450 power supplies to transform a constant-current input into a plasma welding arc. This modality meant that the Profusion system, which included a welding torch, had the lowest purchase cost while also offering high maximum current limits. Additionally, the Profusion headquarters was locally located which would allow for rapid receipt of service and parts.

Table 3: Comparison of Plasma Arc Welding System Suppliers

Supplier	Price	Max Current	Communication	Operational Mode
Profusion	$12,500	450A @ 100% 500A @ 80%	Analog, Modbus	Power Supply Add-on and Torch
Sanrex	$13,500	233A @100% 300A @ 60%	Analog	Power Supply Only
Precision Welding Technologies	$24,200	400A @ 100%	Analog	Power Supply Only
SBI	$44,000	390A @ 100% 400A @ 70%	Any Fieldbus	Complete System
Fronius	$54,400	350A @ 100% 450A @ 60% 500A @ 40%	DeviceNet	Complete System
Liburdi Dimetrics	$167,200	600A @ 100%	Modbus TCP/IP	Complete System

For the second system, the options from Fronius, Liburdi Dimetrics, and SBI were considered with the SBI system being the final selection. The Liburdi system was eliminated immediately due to its high cost and the 600A maximum current was considered unnecessary for the project requirements. Finally, the SBI system was selected over the Fronius option due to its ability to integrate Ethernet/IP communications while the Fronius system was limited to the DeviceNet protocol.

2.3.3 System Integration

To maximize efficiency in testing the systems for tungsten deposition, the GTAW system was integrated onto robot 1 in the MedUSA cell and the plasma systems were tested on robot 2. All systems were integrated into the existing Labview-based control architecture on MedUSA to enable seamless control regardless of the deposition process utilized. After analyzing cooling requirements, it was determined that all systems could utilize the existing Lincoln CoolArc 55 chillers to prevent the GTAW and PAW torches from overheating. For the wire feeding requirements, the GTAW system and Profusion plasma console were integrated with a cold wire feed from the existing Lincoln 4R220 wire feeders while the SBI system would require integration with their SBI WF-1 wire feeder. Apart from the typical installation considerations, the other major modifications to the MedUSA system included modifications to the gas supply system, electrical connections for the Profusion plasma console, and integration of the required control functions into the Labview environment.

2.3.3.1 Gas System Modifications

Unlike the existing GMAW systems integrated on MedUSA, plasma arc welding requires two independent supplies of inert gas. One supply of pure argon to generate the plasma stream and a separate supply for the shielding gas mixture corresponding to the material being deposited. To accommodate this need, two three-way valves were installed on the existing gas supplies for robots 2 and 3 in the MedUSA cell. When configured for plasma welding, the robot 2 line supplies the plasma shielding gas while the robot 3 line supplies the plasma arc gas. Additionally, a solenoid was added to the gas supply for robot 1 to allow for control of the GTAW shielding gas. In the GMAW setup, the gas flow is controlled by a solenoid in the wire feeder, but the configuration of the GTAW bundle required gas flow to be controlled by an independent solenoid.

2.3.3.2 Profusion Plasma Console Signals and Wiring

To incorporate the Profusion Plasma Console into the existing MedUSA system, additional analog components had to be integrated to allow for communication between the plasma console and the existing Labview control interface for MedUSA. This communication was facilitated by an NI cRIO with an appropriate set of modules to interface with the analog I/O utilized for plasma console communication. An overview of the plasma console signaling and cRIO connectivity is shown in Figure 3. The required modules included an NI 9263 Analog Output Module, NI 9425 Digital Input Module, NI 9482 Digital Relay Module, and NI 9215 Analog Input Module.

The plasma console controls are designed to interface directly with the external power supply. The console sends a 0-10V signal to the welder to control the requested current and closes a dry contact relay to enable the power supply. However, the MedUSA system utilizes Lincoln Electric R450 Robotic welders which communicate directly with the Labview controller using Ethernet/IP. This necessitated the NI cRIO to act as a bridge interface between the plasma console and the R450 welders. The general control paradigm for the plasma console is as follows: the plasma console sends a 0-10V command to set the welding current on the plasma console. To start the welding process, a relay closes the start command circuit. The plasma console then sends a 0-10V signal to the welder which is interpreted by the cRIO and utilized to set the correct welding current on the R450 power source. Finally, the plasma console closes the power command circuit when it is ready to weld. The digital input is activated, and the MedUSA interface commands power from the R450. Depending on the plasma console configuration, the plasma welding process is stopped by either releasing the start command or closing the stop command circuit. Additional signals allow the plasma console to indicate when an arc is established and allow the user to test the welding gas or disable the HF pilot arc starter.

In addition to the primary control signals, the plasma console also contains a standard 24V E-stop circuit which disables all plasma console functionality when opened. The E-stop wiring was tied in with the existing E-stop circuitry within the primary MedUSA control box. This prevents any plasma welding from occurring unless the appropriate safety circuits are engaged on the ABB robot controller. After wiring of the plasma console was completed, initial integration testing showed that the NI 9263 Analog Module was susceptible to damage from the high-frequency noise generated by the pilot arc starter on the plasma console. To mitigate this issue, the cabling between the plasma console and cRIO box was replaced with shielded cabling and an additional analog isolation unit was installed.

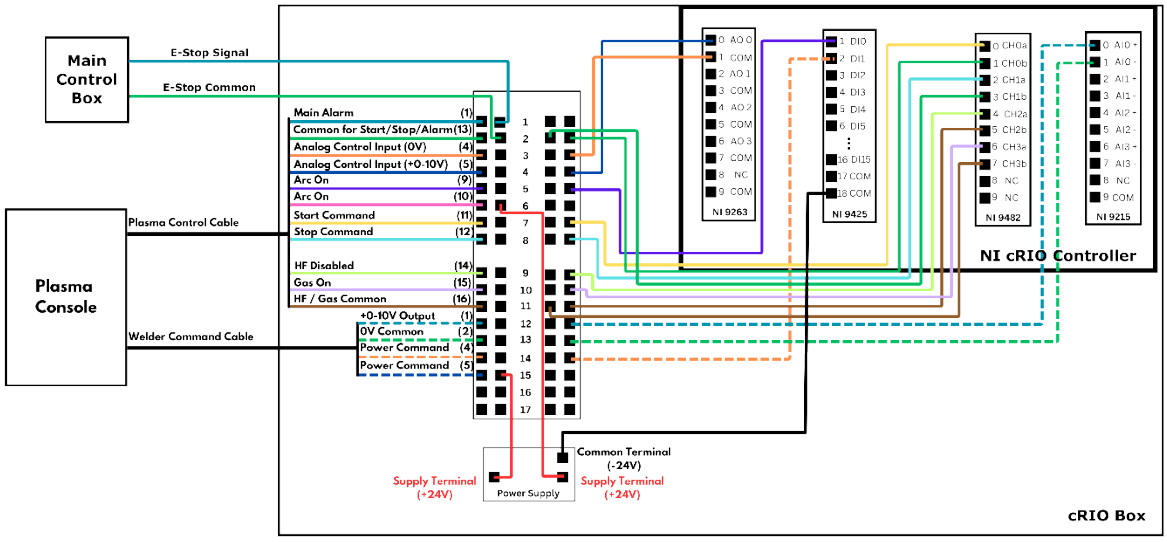

Figure 3. Diagram of the wiring integration of the Profusion Plasma Console

2.3.4 Control Integration

The robot, plasma, and TIG equipment utilizes a modified MedUSA controls architecture. This consists of multiple modules: UI Communication, Welding Equipment Hardware, Print Control, and Robot Execution. The UI Communication is used for interfacing with the controls of the robot and the welding equipment and can also be used to monitor the welding, system state, and robot position feedback. The UI used for the custom robot cell is shown in Figure 4.

Figure 4. Custom Robot Cell Controls UI on the left monitor; Right monitor shows live-view of the robot

Robot and welding parameters can be adjusted on-the-fly, and toolpaths can be loaded and executed using this UI Communication. The Robot Execution Module is used for sending commands to the robot controller to execute certain routines such as commanding full control over the robot and executing maintenance routine paths. The Print Control Module is used to plan and execute the robot motion based on the provided toolpath and deposit the material using the desired welding equipment hardware. The Welding Equipment Hardware Modules consist of three different modules: Lincoln Electric Power

Source, Profusion Plasma Console Controls, and SBI. The Profusion Plasma Console Controls module uses DIO and AIO signals to communicate with the Profusion Plasma equipment. This module also interfaces with the Lincoln Electric Power Source Module by sending welding requests to it. This notifies the Lincoln Electric welder to send the appropriate voltage and current to the Profusion Plasma equipment. Additionally, this module controls the shielding gas and the wire feeder. The Profusion Plasma Console Controls Module is shown in Figure 5 and Figure 6.

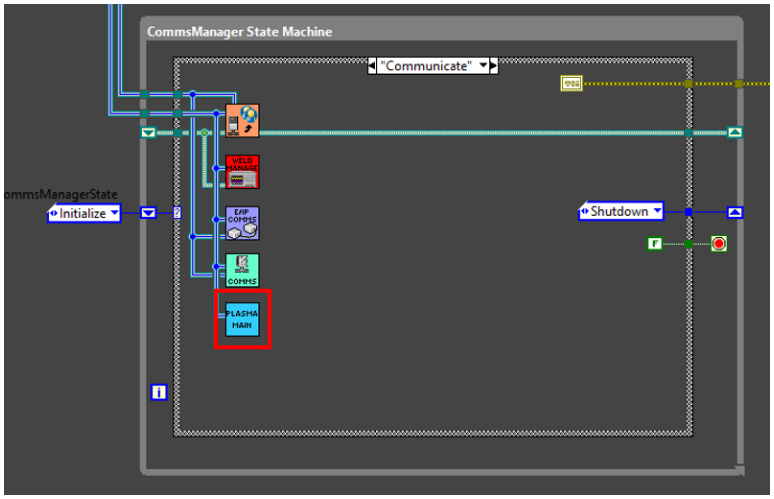

Figure 5. Profusion Plasma Console Controls Module

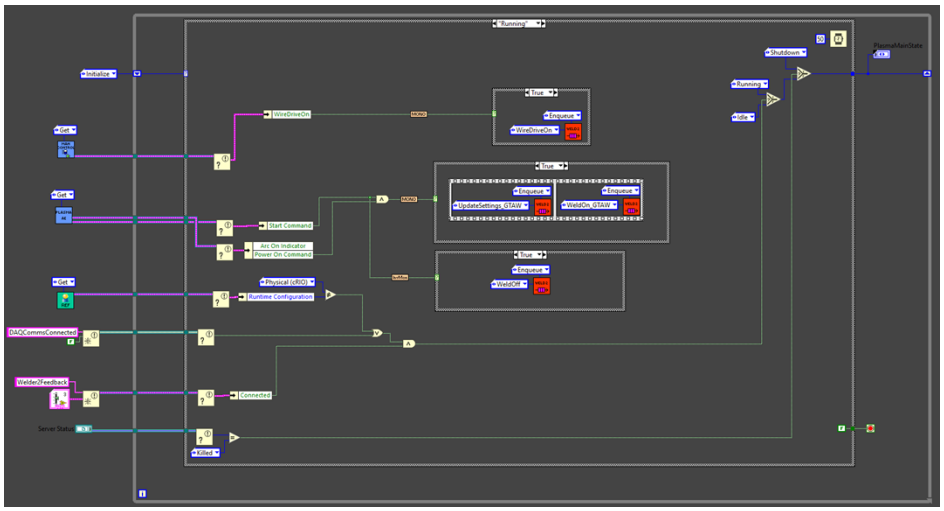

Figure 6. LabVIEW program to request welder commands called from the Plasma Console Controls Module

The TIG equipment is only controlled by the Lincoln Electric Power Source Module. This utilizes the Arclink XT protocol to send requests to the welder and the wire feeder. The SBI module communicates via Ethernet/IP to send commands to the SBI Plasma welder. All automation is achieved using the Print Control Module. The general automation workflow starts off with confirmation that the desired welding equipment used is communicating with the main controller. Once confirmed, the robot moves to the start the desired path, purge gas, and send out an arc command. When an arc is established, the robot will begin movement, and the operator can decide when to feed the wire. After finishing the path, the welding equipment will stop the arc, and the robot moves back to the home position.

2.4 410 SS SYSTEM TESTING

2.4.1 Parameter Development and Initial Deposition

Initial testing was performed utilizing the Abicor-Binzel GTAW torch and the Profusion PAW system. For both systems, these tests followed a similar progression of creating a stable weld pool, adding welding wire to deposit single beads, and then overlapping multiple beads to create a solid layer. Multiple settings were adjusted to determine a suitable operating window before moving to the next step in the process. For the PAW system, it was determined that the stability of the welding process was highly sensitive to standoff distance between the substrate and the plasma torch. As shown in Figure 7, with the plasma torch offset 8mm from the substrate, the melt pool is highly unstable and the molten metal forms bridges across a deep channel formed in the substrate. However, when the offset is lowered to 4mm, this bridging effect disappears, and a stable melt pool is formed which heats the steel substrate without otherwise deforming its geometry.

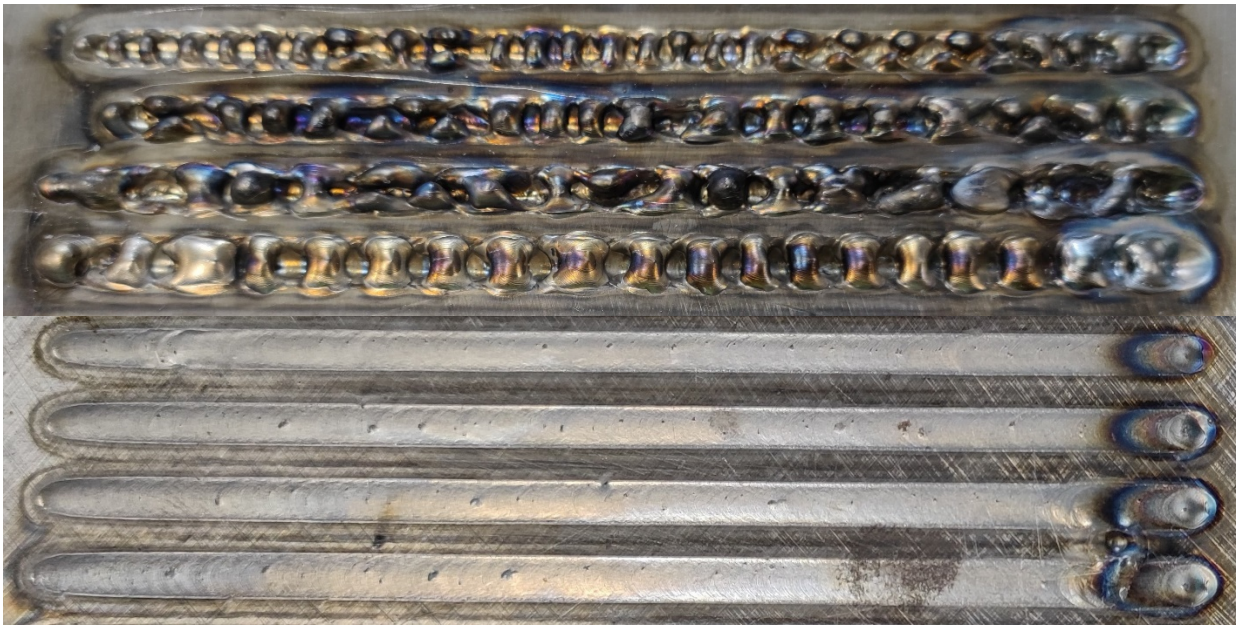

Figure 7. Poor melt pool stability with PAW torch positioned 8mm from the steel substrate (Top) and Stable melt pool with Paw torch 4mm from the substrate (Bottom).

Once the formation of a stable melt pool in a steel substrate was achieved, the next step was to add the cold wire feed and deposit material. The initial welding parameters selected for the first deposition were selected by reviewing the melt pools generated in the previous step and are shown in Table 4. Four beads were deposited with increasing currents and compared as shown in Figure 8. With all welding current above 125A, the beads were similarly stable, but the amount of visible oxidation increased with the increasing heat input. However, it was observed that the steel beads deposited with plasma were generally shiny with low amount of oxidation and there was also minimal spatter compared to the nominal GMAW process.

Table 4: Initial PAW parameters for depositing 0.035" 410 SS wire

Weld Mode	Current	Voltage	Travel Speed	Wire Feed	Gas Mixture
Constant Current	125-150 A	25 V	1.5 mm/s	30 mm/s	100% Ar

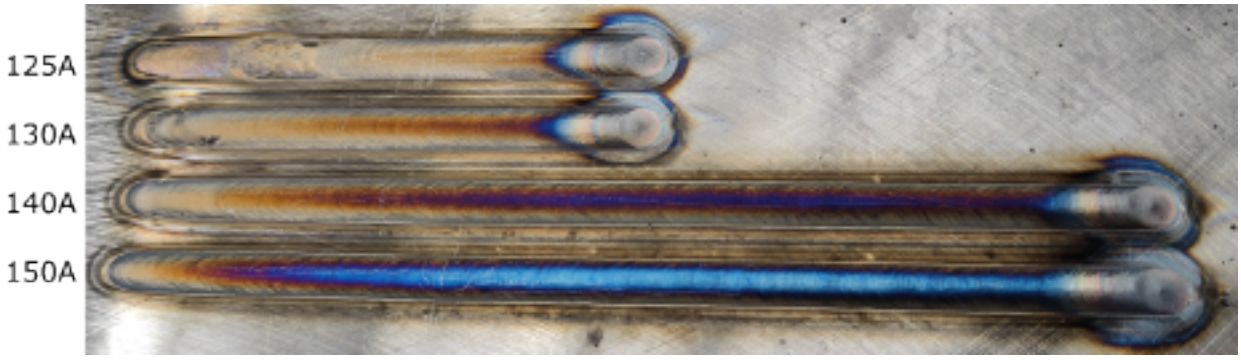

Figure 8. Initial deposition of 410 SS with Profusion Plasma Console.

2.4.2 Resurfacing and Repair

One of the potential concerns when depositing tungsten for the repair of plasma facing components is the typically high surface roughness of material deposited utilizing the WAAM process. However, unlike GMAW, the GTAW and PAW processes can strike an arc and generate heat without depositing material. Combined with robotic welding and appropriate tool path planning, these processes can potential be utilized to improve the geometrical properties of previously deposited beads. WAAM beads typically exhibit a parabolic shape with small valleys between the crests of each deposited bead. While proper bead spacing is essential to minimizing surface roughness, it is difficult to eliminate most of the roughness during the initial deposition. Reheating the deposited material allows it to flow and fill in the gaps left during deposition. In addition to the resurfacing, there was also interest in the filling of holes machined into a 410 SS substrate. Since the process will eventually be utilized to repair damage to tungsten plates, the goal was to fill an arbitrarily sized hole with welded beads and leave a smooth finish.

2.4.2.1 GTAW Repair and Resurfacing

In order to evaluate the repair potential of the GTAW process, a 0.25” thick 410 SS test plate was machined with multiple slots milled out of the surface. These slots were approximately 60mm x 100mm with a depth of 1.6 mm. For this particular geometry, a parameter window for GTAW was calculated which would allow the slots to be filled with a single layer of overlapping beads. The selected parameters for slot filling are shown in Table 5. Two identical slots were filled with the with the same configuration of 12 beads. An attempt was made to fill the slots as accurately as possible without depositing excess material. One of the slots was left in the as-deposited state and the other was resurfaced utilizing a raster pattern parallel to the initial deposition direction as shown in Figure 9.

Table 5: Parameters for GTAW hole filling with 0.035" 410 SS wire

Weld Mode	Current	Voltage	Travel Speed	Wire Feed	Gas Mixture
375	175 A	15 V	2 mm/s	60 mm/s	100% Ar

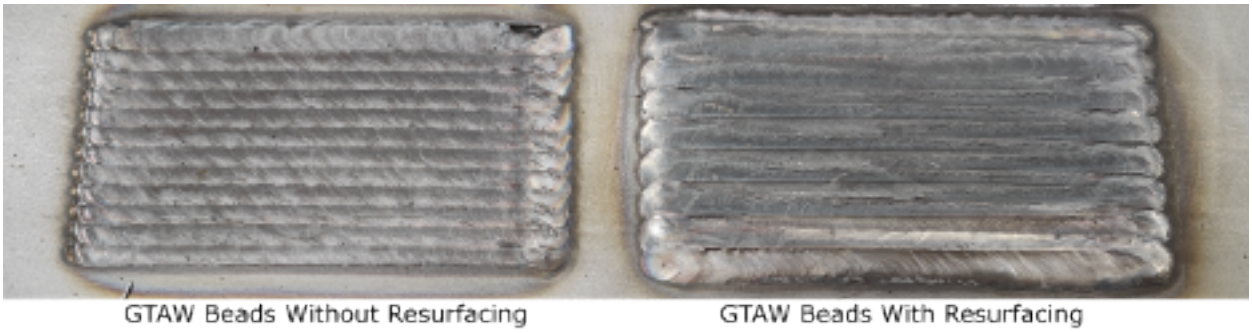

Figure 9: Comparison of beads deposited with GTAW with and without resurfacing.

The parameters utilized for resurfacing the deposited stainless steel beads are shown in Table 6. The spacing between the toolpaths of 4mm ensured that remelted area would overlap slightly with each segment of the raster resurfacing pattern. Note that faster travel speeds were utilized for resurfacing in comparison to the initial deposition as additional heat was generated by the raster pattern and the intent was only to remelt the outer portion of the previously deposited material. After the resurfacing process was completed, the two segments were scanned using a Faro Quantum ScanArm and imported into Geomagic Control X for deviation analysis. Both visually and in the scanned data, it is clear that the resurfacing process removes many of the small inconsistencies of the original deposition and results in more gradual shifts within the deviation map. However, the scanned surface after resurfacing exhibits a slight increase in surface roughness as measured by the standard deviation metric. The deviations greater than 0.5mm can potentially be accounted for by the heat of the resurfacing process warping the 410 SS substrate as this phenomenon could be observed on the edge of the plate near the resurfaced portion. Any future experimentation should employ thicker substrates to alleviate any impact on the measured deviations.

Table 6: Parameters for GTAW resurfacing

Weld Mode	Current	Voltage	Travel Speed	Path Spacing	Gas Mixture
375	175 A	13 V	3.5 mm/s	4 mm	100% Ar

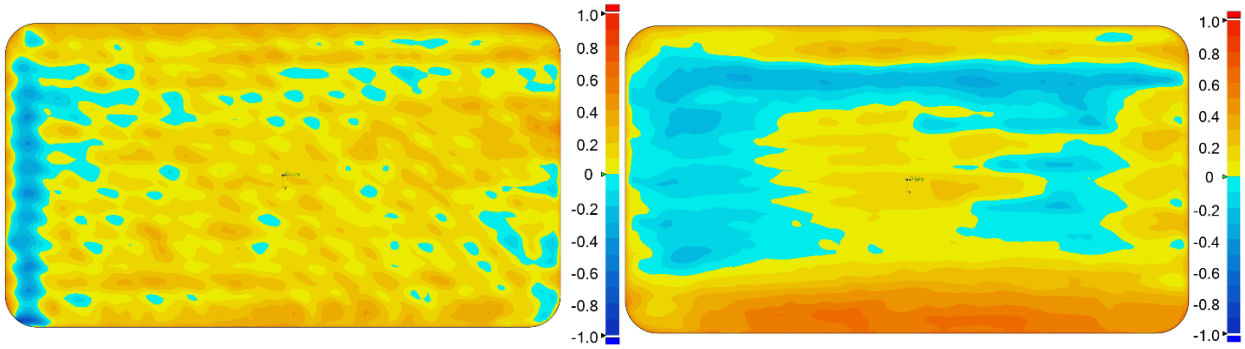

Figure 10: Deviation maps before (left) and after (right) resurfacing with the GTAW torch.

2.4.2.2 PAW Resurfacing

Similar preliminary experiments were conducted on resurfacing utilizing the PAW torch. In this case, no repair was conducted and only a simple resurfacing test was conducted on a square segment of beads deposited via a GMAW torch and 0.035" 410 SS wire. A raster pattern with the toolpath perpendicular to

the original deposition was utilized with parameters for the experiment shown in Table 7. The surface finish of the plate as-deposited and after resurfacing is shown in Figure 11. It is clear from this image that the resurfacing process eliminates most of the original hills and valley though some of the original surface is evident at the edge of the toolpath. This may indicate the need for less space between the raster toolpaths in future experiments. The deviation maps for the plate segments indicated in Figure 11 are shown in Figure 12. Again, while the resurfaced portion exhibits less of the clear horizontally-segmented structure of the original deposition, it actually exhibits a slight overall increase in the measured surface roughness. The existence of higher deviations towards the outer edges of the resurfaced segment may be indicative that the toolpath was not wide enough to completely smooth the surface. The combination of toolpath spacing and heat input may also have been insufficient for optimal resurfacing. The focused heat input of the plasma welding process likely means that a tighter toolpath spacing should be employed in future resurfacing experiments.

Table 7: Parameters for PAW resurfacing

Weld Mode	Current	Voltage	Travel Speed	Path Spacing	Gas Mixture
Constant Current	150 A	25 V	1.5 mm/s	6 mm	100% Ar

Figure 11: Beads that were initially deposited with the GMAW process are resurfaced with the PAW torch.

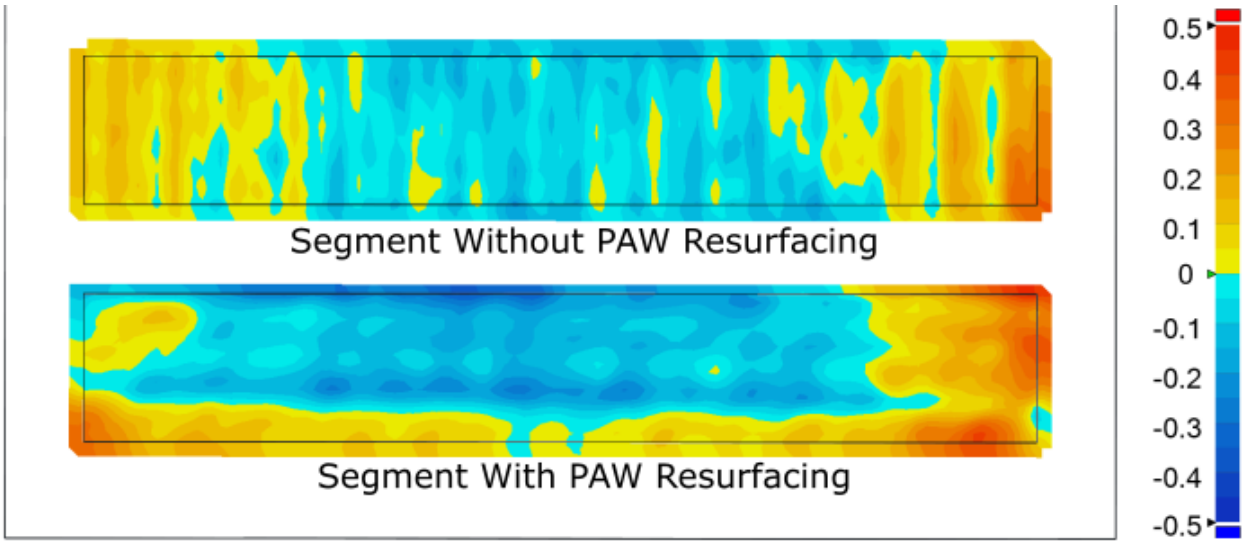

Figure 12: Deviation map of the 410 SS beads deposited with GMAW and the segment resurfaced with the PAW torch.

2.5 CHARACTERIZATION OF METAL DEPOSITION

2.5.1 Characterization Objectives:

The characterization objectives for Year 1 of this effort were to establish a standard operating procedure for examining the cross-section of a TIG/Plasma deposited weld bead. Characteristics of interest include bead profile (height and width), depth of penetration (dilution), depth of HAZ (heat-affected zone), and microstructural defects (pores, cracks, gas inclusions, etc.). After integration of the TIG and Plasma systems within the MedUSA system was completed, preliminary tests of the systems were carried out using 410 stainless steel wire on a mild steel substrate, due to the previous experience of the ORNL MDF team working with this material. It was hypothesized that the characterization procedure developed for 410 stainless steel could be used for future tungsten deposited beads, with slight modifications.

2.5.2 Characterization Procedure:

The initial test of the Profusion plasma welding system included the deposition of multiple beads using 0.035” diameter 410SS wire, shown in Figure 13. Beads 1-4 were deposited with weld currents of 125, 130, 140, and 150 A, while travel speed and weld voltage were held constant at 1.5 mm/s and 25 V, respectively. The infill region shown at the bottom of the image featured a constant current at 125 A, but bead spacing was decreased from top to bottom.

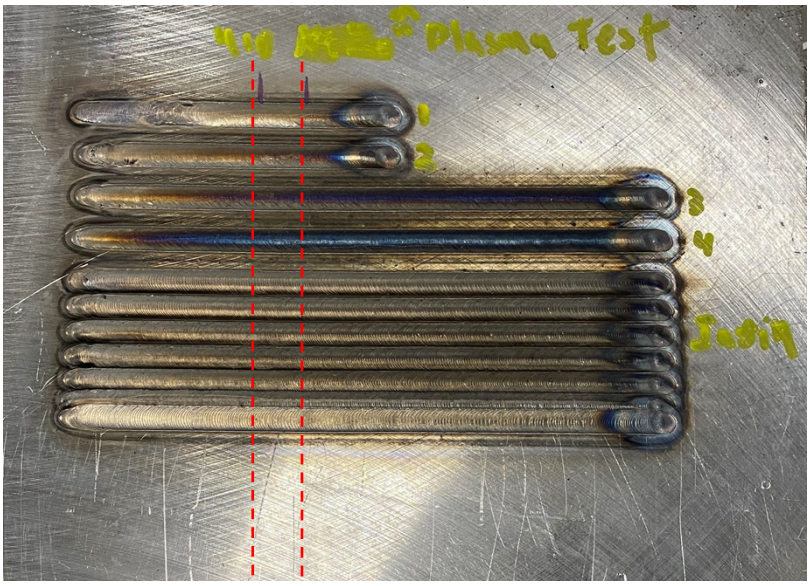

Figure 13. Plasma deposited 410SS beads.

Standard metallographic sample preparation procedures were followed for the plasma deposited weld beads including sectioning, mounting, and polishing of the welds, followed by optical microscopy. First, a 10 mm wide strip including portions of each weld bead was removed from the plate using a horizontal bandsaw, by cutting approximately along the red dotted lines shown in Figure 13. Next, each individual weld bead was sectioned away from each other using a wet saw. Once the samples were individualized, they were hot mounted in Konductomet resin using a SimpliMet automatic mounting press. Beads 1-4 were mounted in a 1.25" diameter puck, while the two groups of infill beads were mounted in a 50 mm diameter puck. Once the samples were mounted, they were ground using 500, 800, 1000, and 2000 grit SiC paper for 1 minute per disc using a Buehler AutoMet 300 Pro. After grinding the samples, they were polished using the procedure outlined in Table 8. Samples mounted in the 50 mm puck were polished for an additional 2 min per step to achieve uniformity/mitigate scratches. The mounted and polished weld beads are shown in Figure 14.

Table 8. Polishing procedure for 410SS samples

Surface	**Abrasive**	**Time (min.)**	**Head RPM**	**Platen RPM**	**Rotation**	**Force (N)**	**Lubricant**
MD-Allegro polishing cloth	6 µm diamond	8	150	150	COMP	30	DP-Purple
MD-Largo polishing cloth	6 µm diamond	8	150	150	COMP	15	DP-Purple
MD-Dac polishing cloth	3 µm diamond	8	150	150	COMP	30	DP-Purple
MD-Nap polishing cloth	1 µm diamond	8	150	150	COMP	30	DP-Purple
MD-Nap polishing cloth*	0.5 µm diamond	8	150	150	COMP	30	DP-Purple

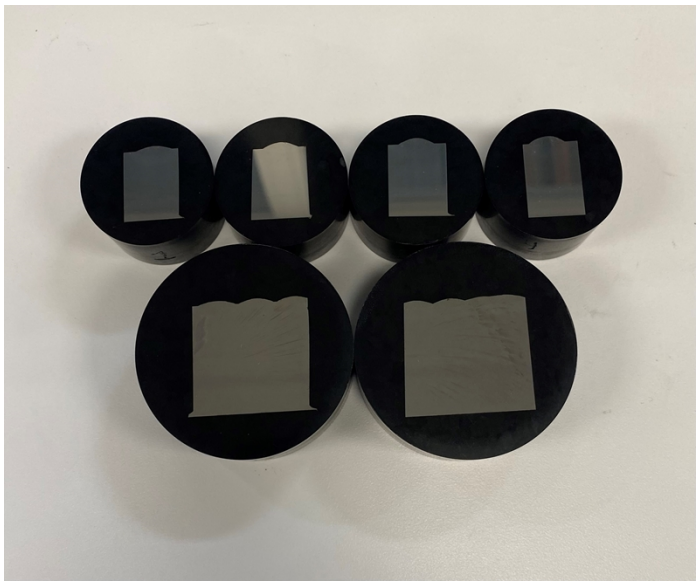

Figure 14. Mounted and polished plasma-deposited 410SS weld beads.

After polishing, the deposited 410SS samples were etched using a modified Fry's etchant to reveal important microstructural features. The etchant consists of 150mL distilled H2O, 50mL HCl, 50mL HNO3, 1g CuCl and each sample was immersed for 5-7 seconds each. Multiple immersion times were attempted to reveal the grain structure while not over etching the samples. Micrographs of the samples were taken at 5X magnification using a Leica DM4000M optical microscope. A Zeiss optical profilometer was used to measure physical characteristics of the weld beads, including bead width, bead height, depth of penetration, and depth of HAZ. Images of polished weld cross-sections for beads 1-4 are presented in Figure 15.

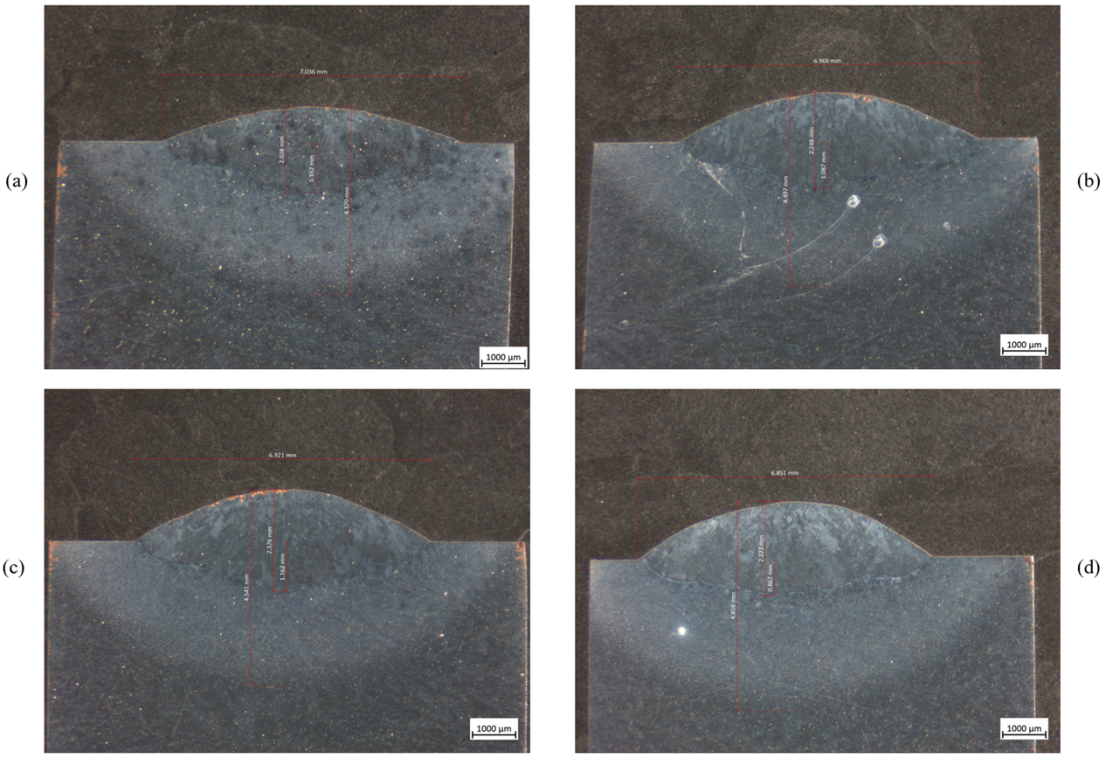

Figure 15.Micrographs of plasma-deposited 410SS weld beads at currents of (a) 125 A, (b) 130 A, (c) 140 A, and (d) 150 A.

2.5.3 Characterization Results

The measured bead width, bead height, depth of penetration, and depth of HAZ for each weld current is presented in Figure 16. After polishing and etching the samples, important features of the weld cross-section such as the fusion zone, heat affected zone, and defects such as pores are easily identifiable. While some aspects of the above procedure such as polishing times, head force, and the etchant used may need to be modified for tungsten, a similar procedure for characterizing tungsten samples deposited using either a TIG or plasma deposition head can be employed.

A trend is observed for the profile of the deposited plasma weld beads, as bead width tends to decrease with an increase in weld current, whereas bead height tends to increase with an increase in weld current. No correlation was observed between depth of penetration or HAZ with weld current; however, measuring the bead profile at additional locations along the weld bead would result in a more accurate conclusion.

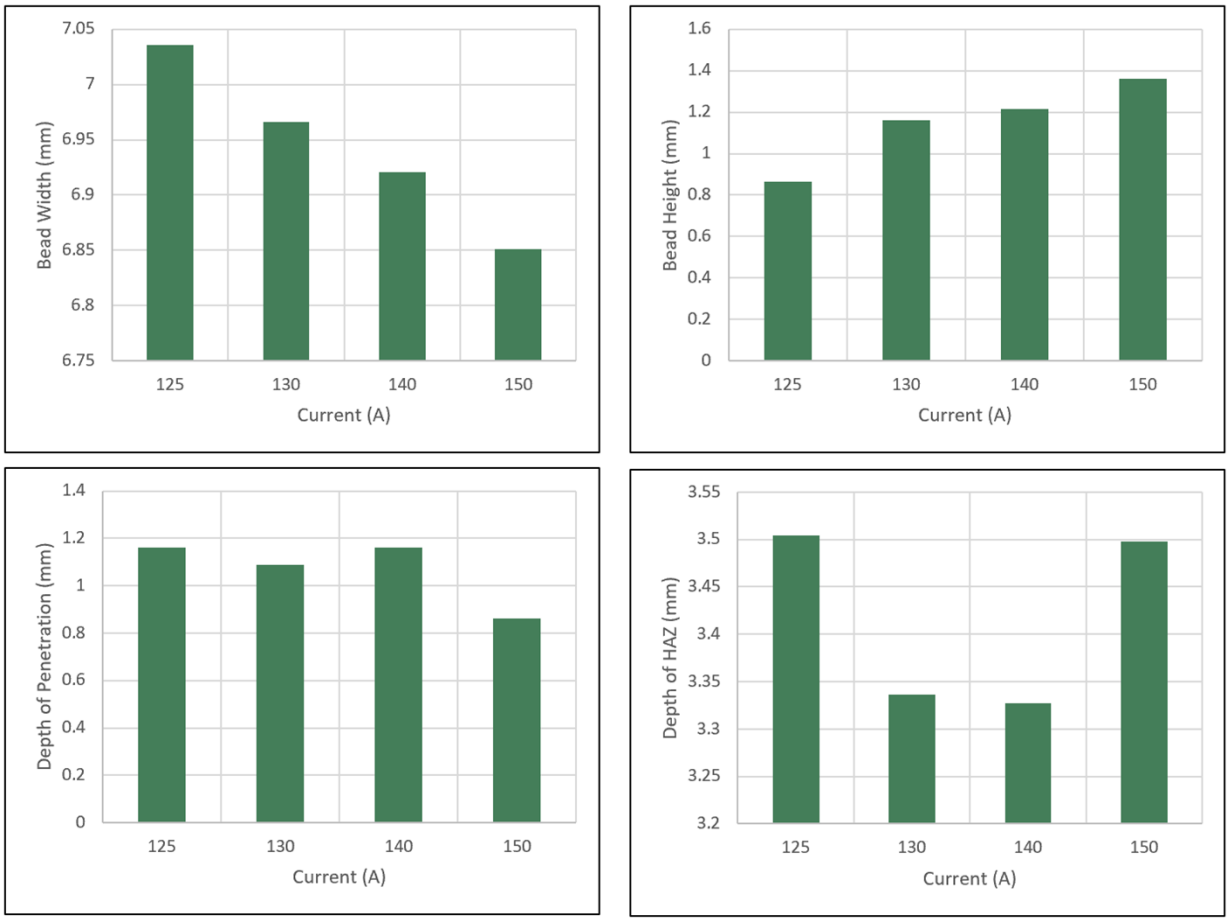

Figure 16. Measurements of bead profile for weld beads deposited at different currents.

A micrograph of bead 4 taken at 5X magnification, with additional images taken at 20X magnification of the fusion zone (top-right), the fusion-HAZ interface (bottom-right), and the HAZ-substrate interface (bottom-left) is presented in Figure 17. The martensitic microstructure of 410SS is clearly observed in the fusion zone, with long needle like grains. Other observations include dark spots which could potentially be carbides that are present in the material or gas inclusions. There are small microcracks observed at the base of the fusion zone in the fusion-HAZ interface, as well as few small pores (~10 µm) in the top of the HAZ. Looking further down into the substrate, there is a higher density of pores in the material with

much larger pores (~30 µm) observed in the substrate compared to the HAZ or fusion zone. This is likely a result of impurities within the substrate material or dissimilarities between the substrate and wire composition.

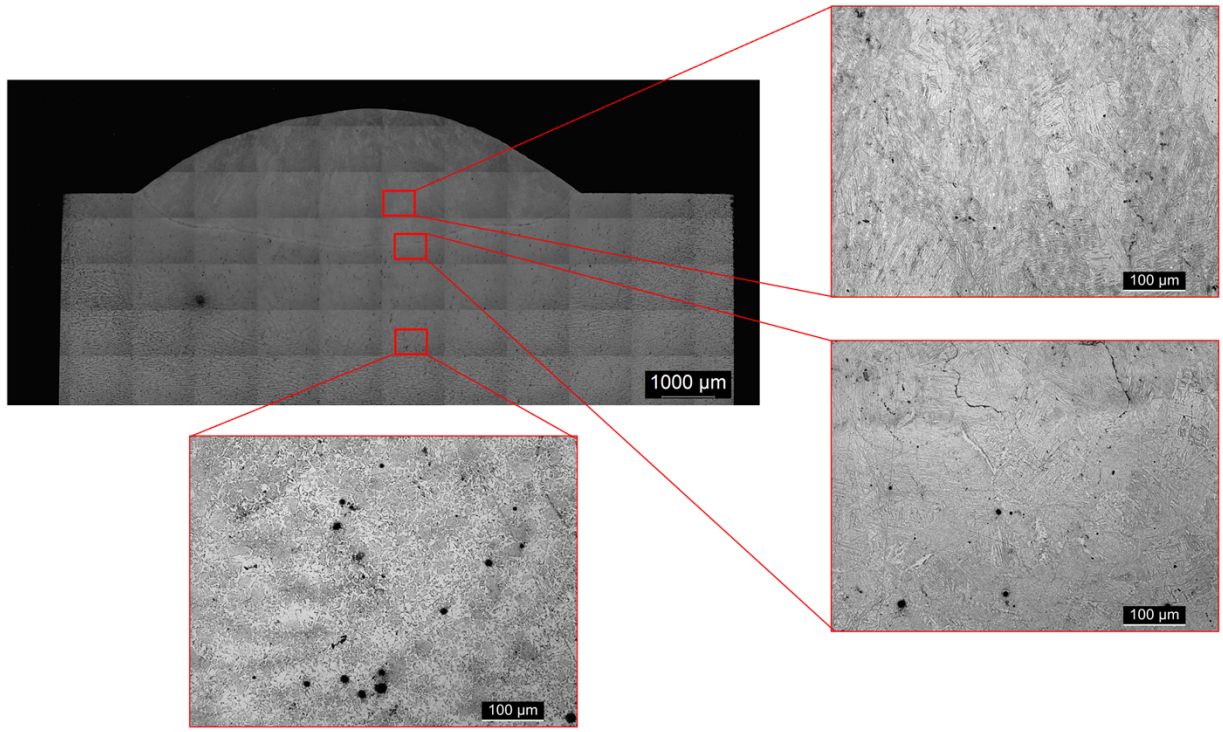

Figure 17. Micrographs taken at 20X magnification of the plasma weld bead deposited using a current of 150 A.

3. TEST SETUP

To demonstrate in-situ repairing of the inner surfaces of a Pilot Plant Tokamak PFCs a new robot cell was developed to replicate the geometry of Tokamak outboard blanket (see Figure 18). The objective of the project is to demonstrate AM method ensures for all orientations inside a Tokamak. A fixture test stand was designed to replicate this "C" shape geometry with horizontal floor, positive 45° angle (away surface), vertical surface, negative 45° angle (towards surface) and horizontal ceiling. Fixture plates (6061-T6 pre-punched on 22.5mm grid) are fastened to Aluminum extrusion 90mm x 90mm (6005-T5) frame to achieve these specific positions (Figure 18). These allow for hold down tooling for locating and fixing the AM test tiles.

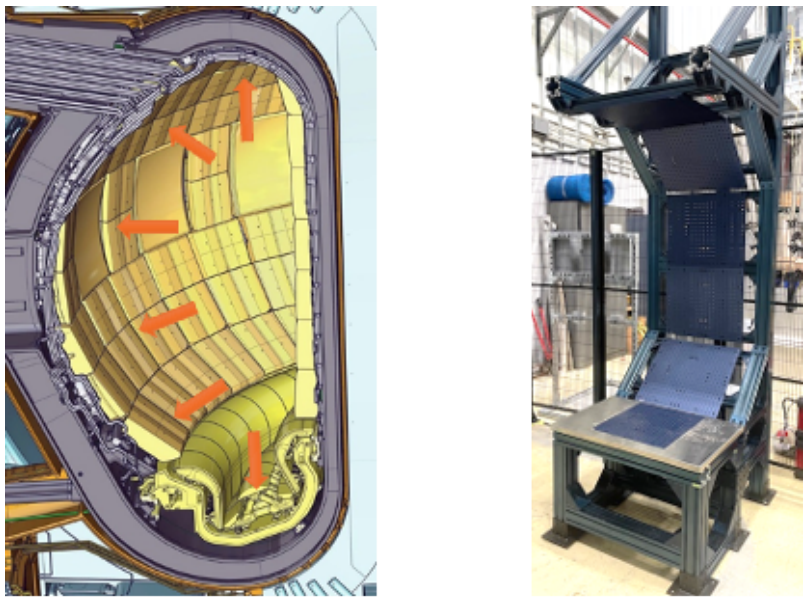

Figure 18 (a) Tokamak Cross-section and (b) AM test Stand.

3.1 IN-SITU REPAIR ROBOT WORKCELL

The AM robot work cell follows the design principals of the ANSI Safety Requirements for Industrial Robots and Robot Systems (ANSI/RIA R15.06-2012). This Standard sets out key points that include keeping employees outside the robot's work area, using proper lockout/tagout procedures, interlinking the robot's programming with all safety devices.

It was determined that the ABB 6-axis robot, that will interface with the AM Test Stand, required a safety enclosure that is 15 foot long by 12 foot wide by 7.25 foot high with full sided arc flash shield curtain (See Figure 19). Other support systems include the TIG wire feeder, operator workstation, TIG power wave unit, and cooling loop, TIG control panel and control pendant, master power supply and Argon gas supply.

Figure 19. WorkCell safety enclosure and support systems.

Gas lines, Wire feed, and power enter the work cell through the openings under or above the enclosure (see Figure 20).

Figure 20 ABB robot with the TIG welder inside the enclosure.

3.2 TEST TILE

Although the project is for studying Tungsten deposition, initially, wear-resistant 410 Stainless Steel (ASTM A240) 0.25" thick plate was used as a test tile (Figure 21d). The melting point of this alloy is between 1,404-1440°C. The temperature of a TIG weld arc can range from 2,760-11,000°C. The Test Tile has slots and pockets milled on top surface to simulate a "2 mm fill-in" repair.

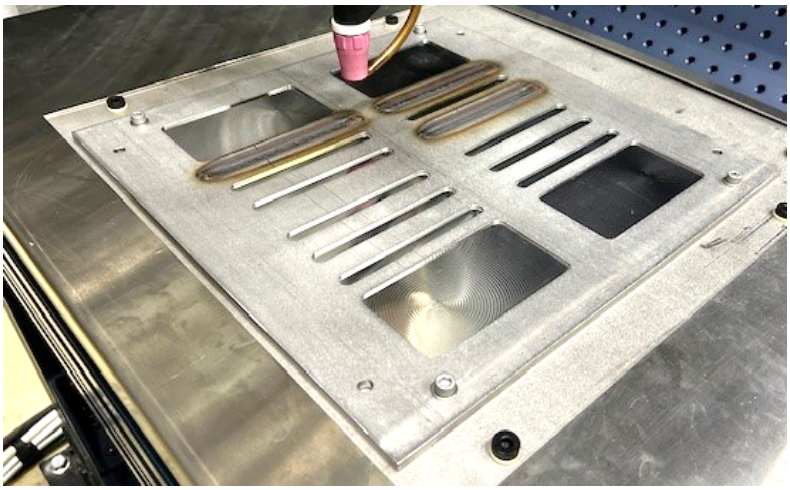

Figure 21. 410 SS Test Tile - Slotted and Pocketed.

3.3 TEST TILE FIXTURING

The material properties of the fixturing components to secure test tile were specified to withstand the TIG arc weld temperatures. Figure 22 shows the properties of the material and their stack up.

Component	*Material*	*Melting Point*
Socket Head Cap Screw	316 SS	1390°C
Test Tile	410 SS	1440°C
Base Plate	304 SS	1421°C
Socket Head Cap Screw	316 SS	1390°C
Sleeve Washer	Ceramic	2000°C
Heat Shield Grid	Sintered Silicon Carbide	2545°C
Splash Shield	304 SS	1421°C
Test Stand Frame	6061-T6 Al	651°C

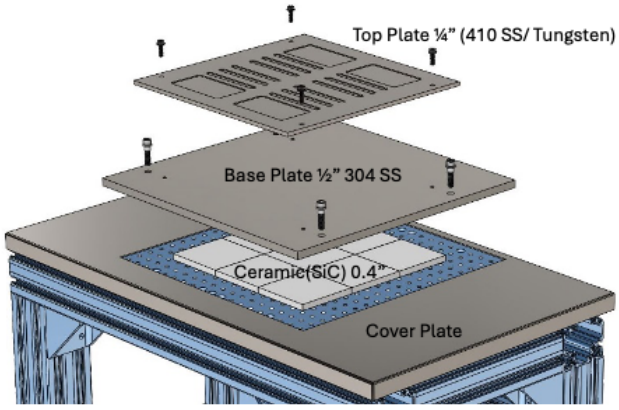

Figure 22 Fixture stack up and their melting points.

The top plate is a consumable and gets changed according to the experiment we will be conducing. Although slots and pockets are milted initially, once experience is developed depositing material in straight slots, more complex geometry deposition will be pursed.

4. FUTURE WORK

During the first year, we selected the specific approach of using the TIG and Plasma consoles. They were integrated into the Lincoln Electric power wave module. After initially testing with TIG torch, successful deposition of material using the plasma torch was performed. Plasma module was also used to refinish the surface of the deposited material.

The objectives for Year 2 are:

1. ***Tungsten AM Deposition***: After being successful in depositing 410 SS in Year 1, Year 2 will be devoted to Tungsten. Modifying the established characterization procedure for plasma deposited 410SS samples to properly analyze TIG or plasma deposited tungsten weld beads. The physical and thermal properties of tungsten are very different from that of 410SS and are outlined in Table 9. A higher thermal conductivity and lower CTE of tungsten will make it more difficult to keep the substrate heated and control cooling rates, likely adding residual stress and making the welds more susceptible to cracking. However, depositing pure tungsten wire on a pure tungsten substrate should reduce the presence of impurities that were causing porosity and inclusions in 410SS.

Table 9. Comparison of physical and thermal properties of 410SS and tungsten [10].

Property	**410SS**	**Tungsten**
Density (g/cm^3)	7.80	19.3
Thermal Conductivity (W/m*K)	24.9	170
Specific Heat (J/kg*K)	460	134
CTE (µm/m/°C)	9.9	4.5
Melting Point (°C)	1480-1530	3410

2. ***Inclined Deposition***: After being successful in depositing the material in the horizontal position, inclined deposition will be pursued. At least 45-degree incline and 90-degrees will be pursued in Year 2.
3. ***Surface characterization***: To determine where the erosion of metal happened in a Tokamak the surface of the PFC will initially be scanned using an optical laser scanner. This will determine where the metal needs to be deposited. To ensure that the deposited layer has < 50 mm surface roughness, a second scan is performed after metal deposition is made. The optical scanner will be a detachable attachment at the ABB robot end effector. The end effector can either pick the plasma head or the laser scanner. This system will be developed in Year 2.
4. ***Resurfacing***: Once the metal layer has been deposited, the surface usually will have parabolic shape. To make this flat and provide a good surface finish, plasma head will be used to remelt the deposited bead and using the cover gas to spread the molten bead to flow into the smaller troughs created during deposition. Our research will focus on the power of the plasma during this process, the end effector speed, standoff distance, cover gas pressure and spread to achieve this.

5. REFERENCES

[1] National Academies of Sciences, Engineering, and Medicine. 2021. Bringing Fusion to the U.S. Grid. Washington, DC: The National Academies Press. https://doi.org/10.17226/25991.
[2] Maisonnier, D.; et al., "DEMO and fusion power plant conceptual studies in Europe", Fus. Eng. Des. **81** (2006) 1123.
[3] Kessel, C.E.; et al., "Overview of the fusion nuclear science facility, a credible break-in step on the path to fusion energy", Fus. Eng. Des. **135** (2018) 236.
[4] Friconneau, J.-P., et al., "ITER hot cell-remote handling system maintenance overview", Fus. Eng. Des. **124** (2017) 673.
[5] Fusion Energy Sciences Advisory Committee report on Transformative Enabling Capabilities for Efficient Advance Toward Fusion Energy (2018), https://science.osti.gov/-/media/fes/fesac/pdf/2018/TEC_Report_15Feb2018.pdf
[6] APS DPP-Community Planning Process Report, March 2020, https://drive.google.com/file/d/1w0TKL_Jn0tKUBgUc8RC1s5fIOViH5pRK/view
[7] FESAC Long Range Planning report, February 2021, https://science.osti.gov/-/media/fes/fesac/pdf/2020/202012/DRAFT_Fusion_and_Plasmas_Report_120420.pdf
[8] Harb, M. et al, "Calculation of Shutdown Dose Rate in Fusiuon Nuclear Science Facility During a Proposed Maintenance Scheme", Fusion Sci. Technol., **75**, (2019) 747.
[9] M, G., et al., "Development of wire + Arc additive manufacture for the production of large-scale unalloyed tungsten components", International Journal of Refractory Metals and Hard Materials, Vol 82, August 2019, pp 329-335. (https://doi.org/10.1016/j.ijrmhm.2019.05.009)
[10] "Stainless steel - grade 410 (UNS S41000)," AZoM, https://www.azom.com/article.aspx?ArticleID=970 (accessed Sep. 17, 2024).